



Hydrodynamic Model Description

Scalpay, Inner Sound

CAR/L/1156482

January 2024

Mowi Scotland	OFFICE	PHONE	FAX
	Mowi, Farms Office, Glen Nevis Business Park PH33 6RX Fort William		-
	POSTAL	MAIL	
	Mowi, Farms Office, Glen Nevis Business Park PH33 6RX Fort William	environment@mowi.com	
		WEB	
		http://mowiscotland.co.uk	

CONTENTS

	Page
1. INTRODUCTION	4
2. MODEL DESCRIPTION	4
3. CONFIGURATION AND BOUNDARY FORCING FOR SCALPAY	5
4. MODEL CALIBRATION AND VALIDATION WITH HYDROGRAPHIC DATA	8
4.1 Calibration: January – March 2023, ID409	8
4.2 Validation: August – September 2015, ID054	12
5. MODELLED FLOW FIELDS, AUGUST – SEPTEMBER 2015 (ID054)	15
6. MODEL EVALUATION AGAINST DYE AND DROGUE TRACK DATA	16
6.1 Dye Releases	16
6.2 Drogue Releases	17
7. REFERENCES	19

LIST OF FIGURES

- Figure 1. Location of the salmon farm, Scalpay and the location of the ADCP deployments (▲) relative to the pen positions (o). 4
- Figure 2. The ECLH mesh and domain of the modelling study (SSM) 6
- Figure 3. The unstructured mesh around the Scalpay site in the modified model grid, with the proposed pen locations indicated (O). 7
- Figure 4. Model water depths (m) in the area around the Scalpay salmon farm. The pen locations are indicated (●). 7
- Figure 5. Comparison between observed and modelled sea surface height from January – March 2023 (ADCP deployment ID409) using model parameter values from Table 1. Both the full record (left) and a subset of 15 days (right) are shown. Observed data are in blue, model results in red. 9
- Figure 6. Comparison between observed and modelled East (left) and North (right) components of velocity at the three selected cell depths at the ADCP location for 15 days in January - March 2023 (ID409). Observed data are in blue, model results in red. 10
- Figure 7. Scatter plot of observed and modelled velocity at each of the three selected cell depths at the ADCP location from January – March 2023 (ID409). Observed data are in blue, model results in red. 11
- Figure 8. Histograms of observed and modelled speed (left) and direction (right) at the three selected cell depths at the ADCP location from January – March 2023 (ID409). Observed data are in blue, model results in red. 12
- Figure 9. Comparison between observed and modelled sea surface height from January – March 2023 (ADCP deployment ID409) using model parameter values from Table 1. Both the full record (left) and a subset of 15 days (right) are shown. Observed data are in blue, model results in red. 13
- Figure 10. Scatter plots of observed and modelled velocity for the three selected cell depths at the nominal ADCP location for August – September 2015 (ID054). Observed data are in blue, model results in red. 13
- Figure 11. Histograms of observed and modelled speed (left) and direction (right) for the three selected cell depths at the ADCP location from August – September 2015 (ID054). Observed data are in blue, model results in red. 14

- Figure 12. Comparison between observed and modelled East (top) and North (bottom) components of velocity for the three selected cell depths at the ADCP location for August – September 2015 (ID054). Observed data are in blue, model results in red. 14*
- Figure 13. Modelled flood (left) and ebb (right) surface current vectors during spring tides. For clarity, only every 10th vector is shown. 15*
- Figure 14. Observed (circles) and modelled (solid lines) dye tracks from the eight releases at Scalpay on the 5th and 6th March 2022. Each release is coloured differently. 17*
- Figure 15. Observed (symbols) and modelled (solid lines) drogue tracks from the eight releases at Scalpay on the 5th and 6th March 2022. The different shaped symbols represent individual drogues. 18*

LIST OF TABLES

Table 1. Parameter values chosen for the FVCOM model during the calibration simulations. 8

Table 2. Model performance statistics for East and North velocity at the ADCP location from January – March 2023 (ID409) for the three selected cells..... 9

Table 3. Model performance statistics for East and North velocity for the three selected cell depths at the ADCP location from August – September 2015 (ID054).....15

Table 4. Details of the dye releases undertaken at Scalpay in March 202216

Table 5. Details of the drogue releases undertaken at Scalpay in March 2022. Note that the drogue release numbers do not correspond directly to the dye release numbers.17

Table 6. Location details for each drogue release18

1. Introduction

This report has been prepared by Mowi Scotland Ltd. to meet the requirements of the Scottish Environment Protection Agency (SEPA) for an application to use topical sealice veterinary medicines at the **Scalpay** marine salmon farms in the **Inner Sound** (Figure 1). The application uses coupled hydrodynamic and particle tracking modelling to describe the dispersion of bath treatments in order to determine EQS-compliant quantities for the current site biomass and equipment. The modelling procedure follows as far as possible guidance presented by SEPA in December 2023 (SEPA, 2023). This report describes the configuration, calibration and validation of the hydrodynamic model used in the application. The dispersion modelling for the site is described in a separate report (Mowi, 2024).

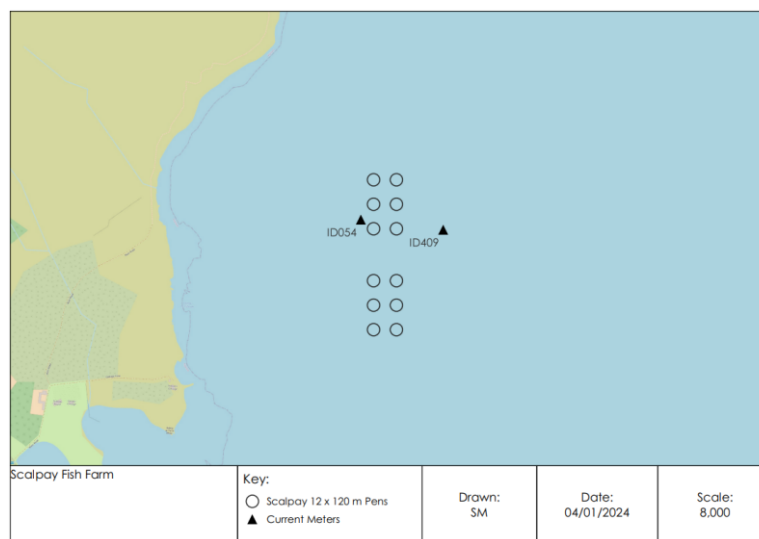


Figure 1. Location of the salmon farm, Scalpay and the location of the ADCP deployments (▲) relative to the pen positions (○).

2. Model Description

The hydrodynamic model used in the particle tracking modelling at Scalpay was FVCOM (Finite Volume Community Ocean Model), a prognostic, unstructured-grid, finite-volume, free-surface, 3-D primitive equation coastal ocean circulation model developed by the University of Massachusetts School of Marine Science and the Woods Hole Oceanographic Institute (Chen et al., 2003). The model consists of equations describing the evolution and conservation of momentum, temperature, salinity and turbulence parameters, the latter using a turbulence closure submodel. The horizontal grid is comprised of unstructured triangular cells and the irregular bottom is presented using generalized terrain-following coordinates. The General Ocean Turbulent Model (GOTM) developed by Burchard's research group in Germany (Burchard, 2002) has been added to FVCOM to provide optional vertical turbulent closure schemes. Horizontal viscosity and diffusivity was calculated using the Smagorinsky algorithm, with a coefficient value c_s . FVCOM is solved numerically by a second-order accurate discrete flux calculation in the integral form of the governing equations over an unstructured triangular grid. This approach combines the best features of finite-element methods (grid flexibility) and finite-difference methods (numerical efficiency and code simplicity) and provides a much better

numerical representation of both local and global momentum, mass, salt, heat, and tracer conservation. The ability of FVCOM to accurately solve scalar conservation equations in addition to the topological flexibility provided by unstructured meshes and the simplicity of the coding structure has made FVCOM ideally suited for many coastal and interdisciplinary scientific applications, such as typically found in Scotland. The mesh flexibility allows greater spatial resolution in near-shore areas without excessive computational demand.

The model is forced by a tidal condition along the open boundary, and by frictional stresses at the surface and seabed. At the seabed, the frictional stress, τ_b , is calculated using a quadratic equation where:

$$\tau_b = \rho C_D \mathbf{U}|\mathbf{U}| \quad (1)$$

where $\rho = 1025 \text{ kg m}^{-3}$ is the water density, \mathbf{U} is the velocity in the layer closest to the seabed. The drag coefficient, C_D , is calculated from the bed roughness lengthscale, z_0 , using:

$$C_D = \left(\frac{\kappa}{\ln \left(\frac{z_b + z_0}{z_0} \right)} \right)^2 \quad (2)$$

where $\kappa=0.4$ is von Karman's constant, and z_b is the height above the bed of the lowest velocity point. The value of z_0 was varied during calibration to provide the best fit to observations of sea level and velocity.

Wind forcing is applied as a surface stress calculated from hourly wind speed and direction. Wind stress is calculated from the wind velocity by a standard quadratic relation:

$$\tau_x = \rho_a C_W u W \quad (3a)$$

$$\tau_y = \rho_a C_W v W \quad (3b)$$

where (u,v) are the East and North components of wind velocity respectively, W is the wind speed ($W = [u^2+v^2]^{1/2}$), ρ_a is the density of air, and the wind drag coefficient C_W is calculated following Large and Pond (1981).

3. Configuration and Boundary Forcing for Scalpay

The unstructured mesh used in the modelling (Figure 2) was adapted from the East Coast of Lewis and Harris (ECLH) sub-model mesh of the Scottish Shelf Model (SSM; Marine Scotland, 2016). The model resolution was enhanced in the Caol Mor region, particularly around the Scalpay site (Figure 3). The spatial resolution of the model varied from 20 m in some inshore waters and round the farm pens to 5 km along the open boundary. The model consisted of 50,730 nodes and 95,530 triangular elements. Model bathymetry was taken from the UK Hydrographic Office, supplemented with a local bathymetry survey which was conducted at the site in August 2015.

The model was forced along its open boundary by a time series of sea surface height (SSH) at each boundary node for the relevant simulation periods; FVCOM appears to perform better with time series boundary forcing than when tidal constituents are used. The SSH time series were generated using the RiCOM hydrodynamic model (Walters and Casulli, 1998; Gillibrand et al., 2016) on the ECLH grid, which was, in turn, forced by eight tidal constituents (M_2 , S_2 , N_2 , K_2 , O_1 , K_1 , P_1 and Q_1) taken from the full Marine Scotland Scottish Shelf Model (SSM; Marine

Scotland, 2016) using the MATLAB® tidal analysis routine `t_tide` (Pawlowicz et al., 2002). Wind speed and direction data were taken from the European Centre for Medium-Range Weather Forecasts (ECMWF 2021), with data interpolated onto the nodal locations of the model mesh.

The model was run in 3D, with 10 sigma layers in the vertical. The sigma levels were closer together near the surface and seabed, with sigma level depths of: $\sigma = [0, -0.02 -0.08 -0.18 -0.32 -0.5 -0.68 -0.92 -0.92 -0.98 -1.0]$. Freshwater discharges were input to the model domain at 155 locations, with the freshwater flux data at each location based on the climatological river flows from the Scottish Shelf Model.

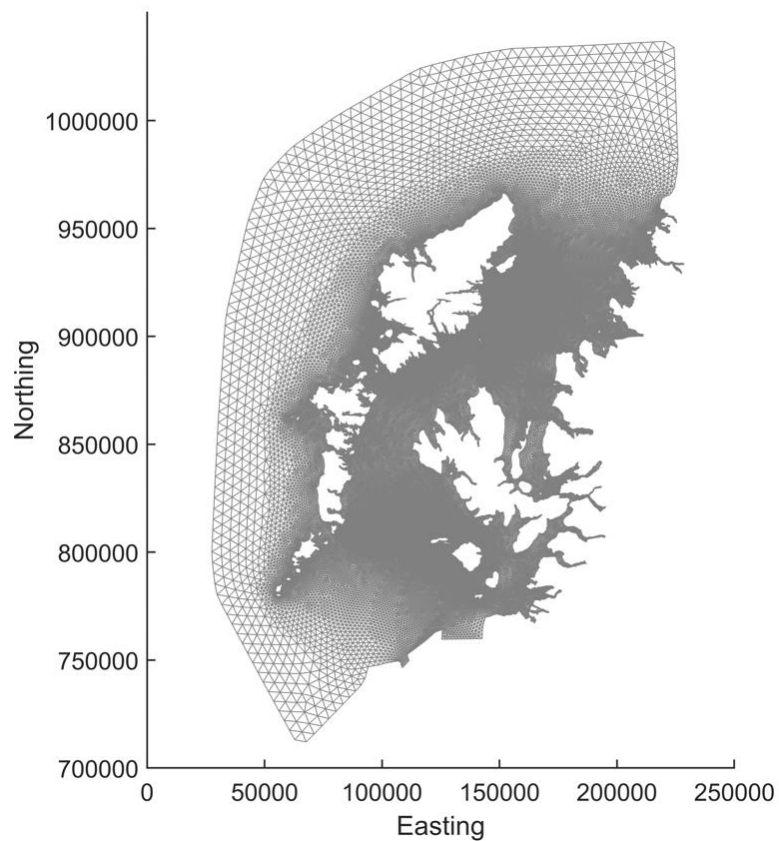


Figure 2. The ECLH mesh and domain of the modelling study (SSM)

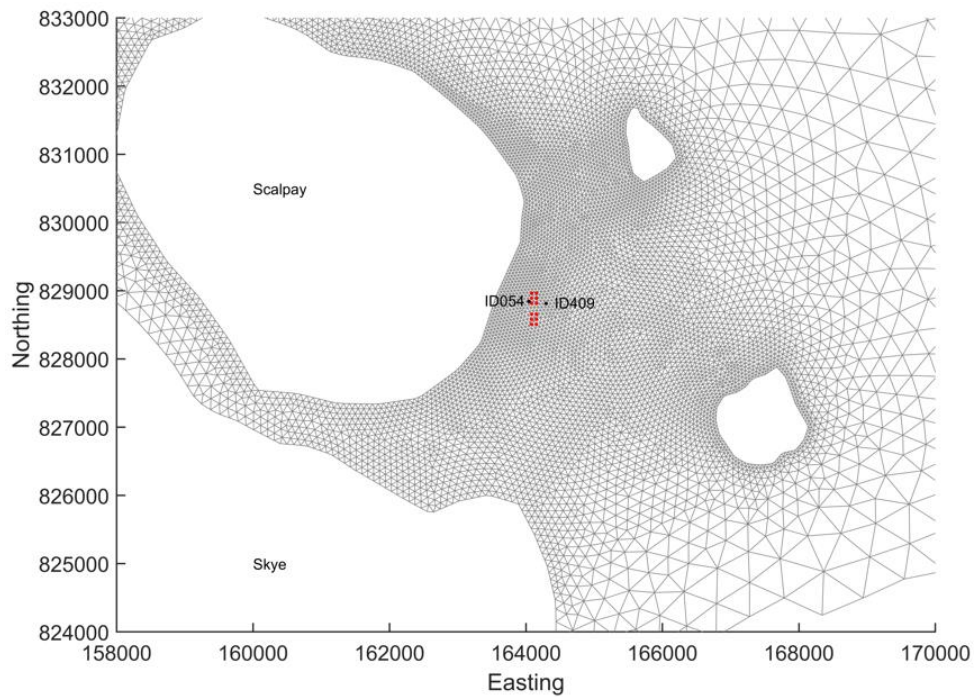


Figure 3. The unstructured mesh around the Scalpay site in the modified model grid, with the proposed pen locations indicated (○).

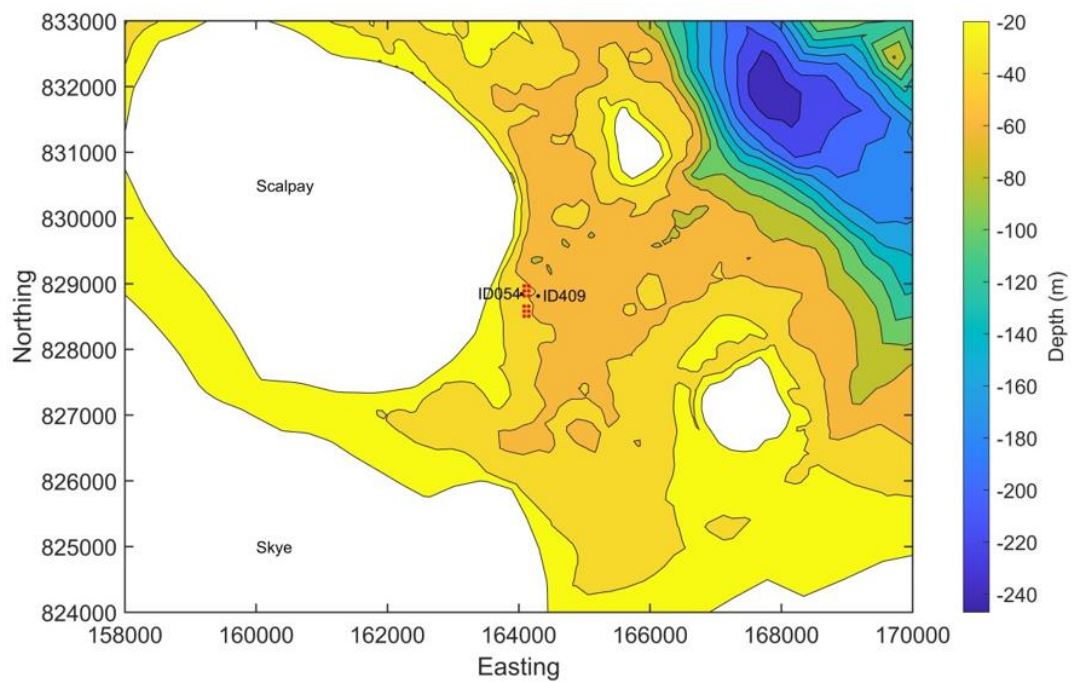


Figure 4. Model water depths (m) in the area around the Scalpay salmon farm. The pen locations are indicated (●).

4. Model Calibration and Validation with Hydrographic Data

For the current study, the FVCOM model was calibrated against hydrographic data collected in the region of the farm site in 2015 and 2023. The data are described in the relevant hydrographic reports. In August 2015, an Acoustic Doppler Current Profiler (ADCP) was deployed close to the farm site (Figure 1) until September 2015 (ID054). In January 2023, another ADCP was deployed close to the site (Figure 1) until March 2023 (ID409). In all, 113 days of current data were used in this application. ADCP deployments provided both current velocity and seabed pressure data, which were used to calibrate and validate modelled velocity and sea surface height. The model was calibrated initially against data from January – March 2023 (ID409), then validated against data from the earlier deployment, ID054.

For each simulation, the model was “spun-up” for three days with boundary forcing ramped up from zero over a period of 48 hours. The model state at the end of the 72-hour spin-up period was stored, and the main simulations “hot-started” from this state.

The following main simulations were performed, corresponding with the dates of the ADCP deployments:

- (i) Calibration: 05 January – 31 March 2023 (ID409, 85 days)
- (ii) Validation: 06 August – 03 September 2015 (ID054, 28 days)

[Note that the dates above refer to the main simulations and that the spin-up simulations ran for three days prior to the start dates given above.]

Model performance is assessed using three metrics: the mean absolute error (MAE), the root-mean-square error (RMSE) and the model skill (d_2). The first two are standard measures of model accuracy; the third, d_2 , is taken from Willmott et al. (1985) and lies in the range $0 \leq d_2 \leq 1$, with $d_2 = 0$ implying zero model skill and $d_2 = 1$ indicating perfect skill.

4.1 Calibration: January – March 2023, ID409

The calibration used observed depth and current velocity from the ADCP location to compare with modelled sea surface height (SSH) and velocity (ADCP deployment ID409). The model was calibrated by varying the value of the bed roughness coefficient, z_0 , in Equation 2, which determines the frictional effect of the seabed on the flow, and the horizontal viscosity and diffusivity coefficient, c_s . After a number of simulations, a final parameter set was selected (Table 1).

Table 1. Parameter values chosen for the FVCOM model during the calibration simulations.

Parameter Description	Value
Bed roughness lengthscale, z_0 (m)	0.01
Horizontal viscosity coefficient, c_s	0.2
Number of vertical layers	10
Barotropic time step (s)	0.5
Baroclinic time step (s)	5.0

The results of the calibration exercise are presented in Figure 5 – Figure 8 and Table 2. At the ADCP location, the sea surface height was reasonably accurately modelled, with model skill of 0.99. The mean absolute error (MAE) and root-mean-square error (RMSE) values of 0.19 m and 0.23 m are about 3.2 % and 3.9 % of the spring tide range (5.95m) respectively.

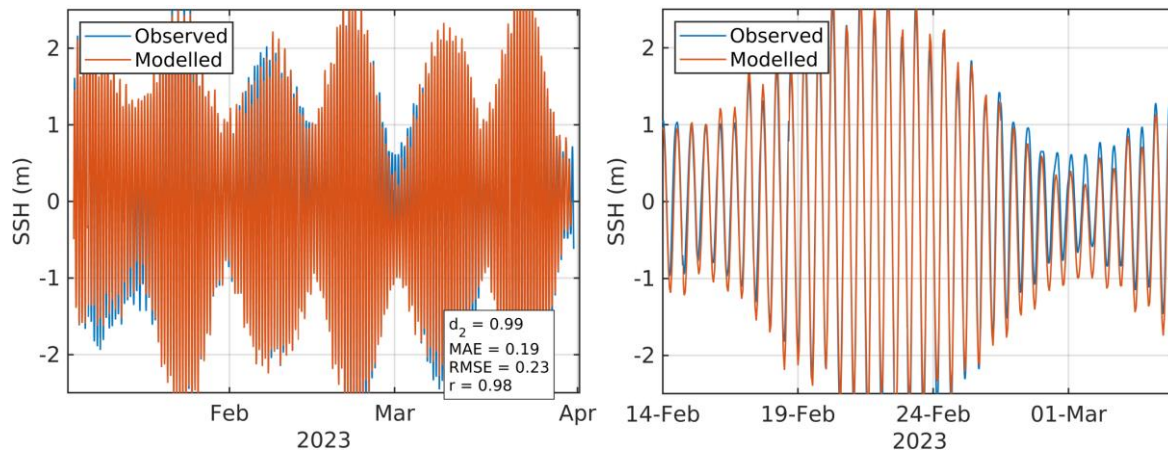


Figure 5. Comparison between observed and modelled sea surface height from January – March 2023 (ADCP deployment ID409) using model parameter values from Table 1. Both the full record (left) and a subset of 15 days (right) are shown. Observed data are in blue, model results in red.

For the calibration period, the model skill scores for the East component were 0.49, 0.50 and 0.48 at the three selected cell depths. For the North component of velocity, the model skill scores were 0.57, 0.64 and 0.62 at the three selected cell depths. MAE and RMSE values were between 0.03 and 0.06 for the two velocity components at the three cell depths (Table 2, Figure 6). The scatter plots and histograms demonstrate that the modelled current had broadly the same magnitude and direction characteristics as the observed data (Figure 7 and Figure 8). The modelled near-bed currents are weaker than the observed, but since bathymetric dispersion occurs in the near-surface layers, where the comparison was better, the weaker near-bed currents are unlikely to impact the bathymetric dispersion simulations.

Table 2. Model performance statistics for East and North velocity at the ADCP location from January – March 2023 (ID409) for the three selected cells.

		East	North
Near-surface cell	Model skill	0.49	0.57
	MAE	0.03	0.05
	RMSE	0.04	0.06
Cage-bottom cell	Model skill	0.50	0.64
	MAE	0.03	0.04
	RMSE	0.03	0.05
Near-bed cell	Model Skill	0.48	0.62
	MAE	0.03	0.03
	RMSE	0.03	0.04

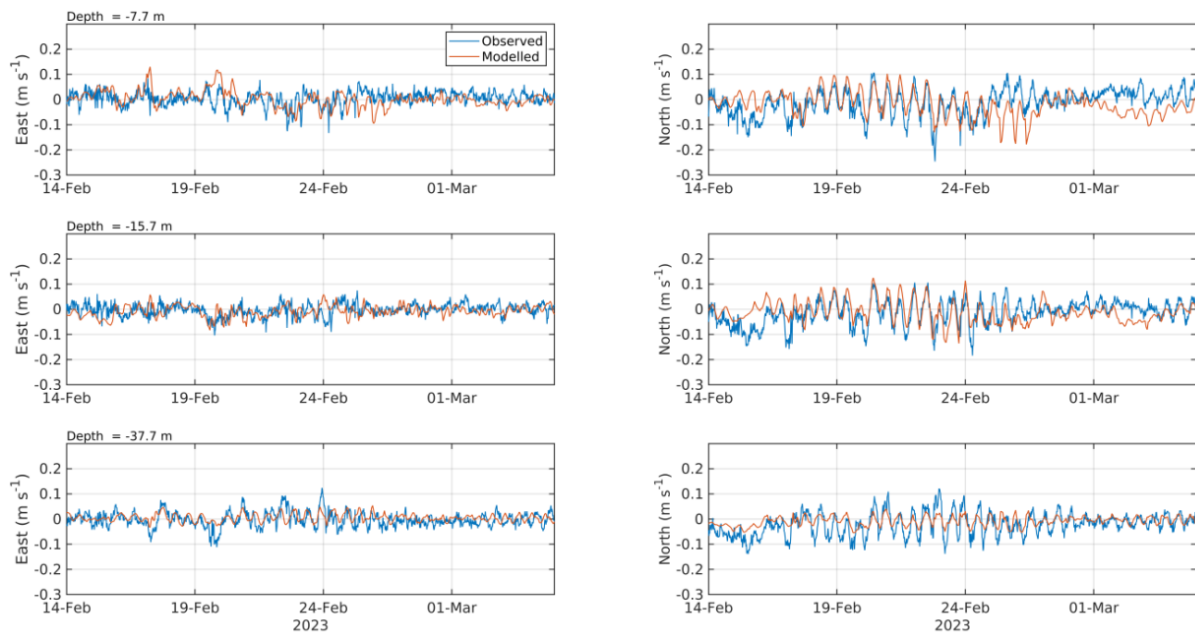


Figure 6. Comparison between observed and modelled East (left) and North (right) components of velocity at the three selected cell depths at the ADCP location for 15 days in January - March 2023 (ID409). Observed data are in blue, model results in red.

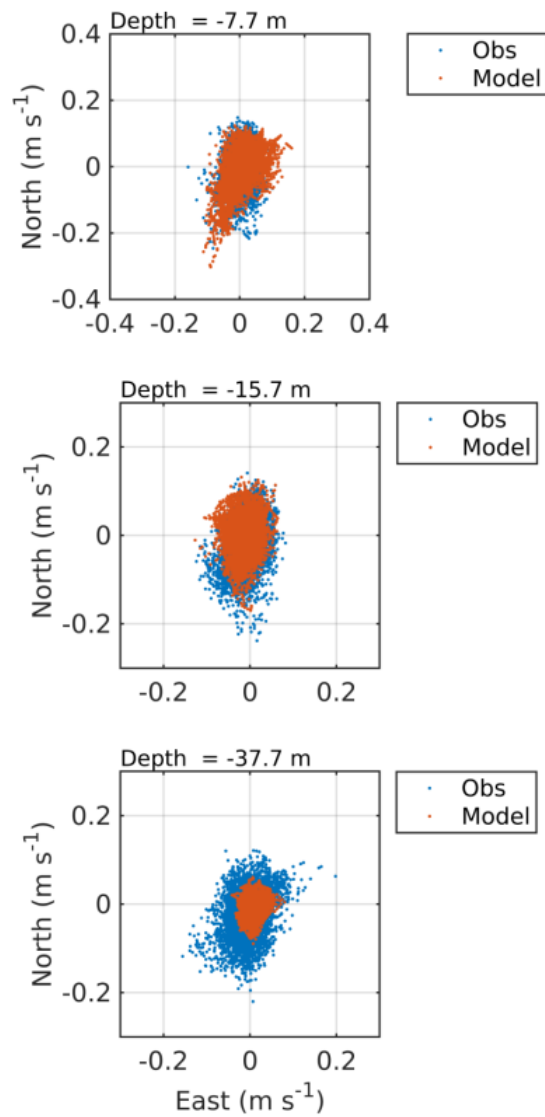


Figure 7. Scatter plot of observed and modelled velocity at each of the three selected cell depths at the ADCP location from January – March 2023 (ID409). Observed data are in blue, model results in red.

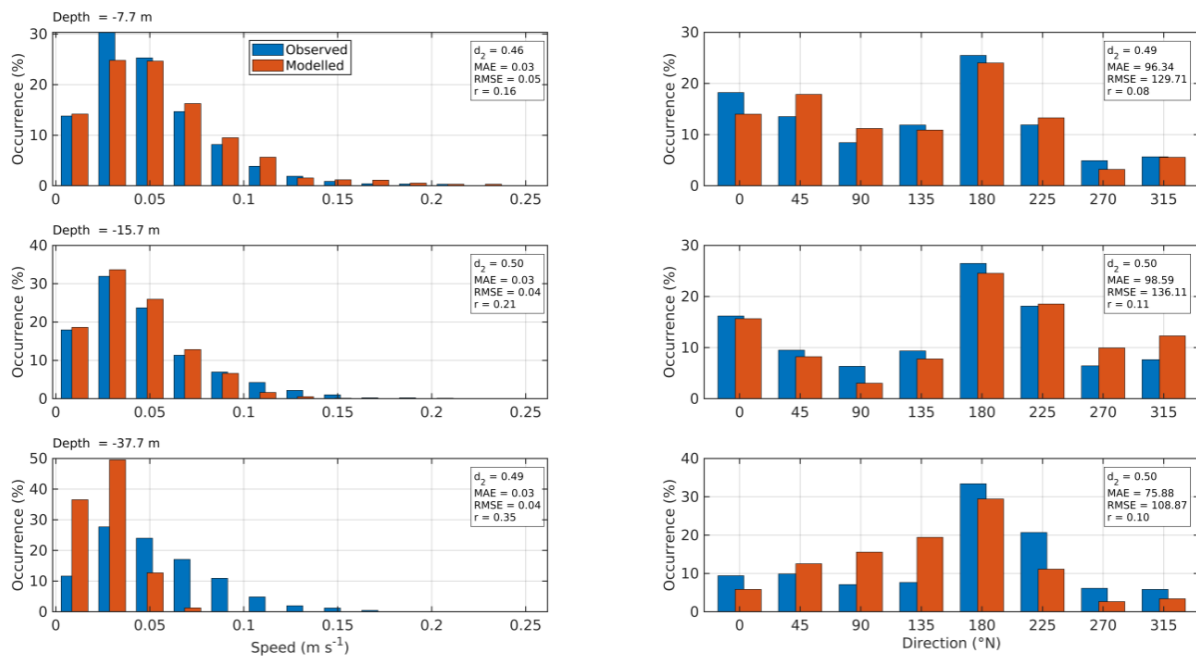


Figure 8. Histograms of observed and modelled speed (left) and direction (right) at the three selected cell depths at the ADCP location from January – March 2023 (ID409). Observed data are in blue, model results in red.

4.2 Validation: August – September 2015, ID054

The model was then validated against a second data set collected at the Scalpay site in September 2015, using the same variables from the ID409 run (ID054). At the ADCP location, the sea surface height was reasonably accurately modelled, with model skill of 0.93 (Figure 9). The mean absolute error (MAE) and root-mean-square error (RMSE) values of 0.56 m and 0.66 m were about 11.3 % and 13.4 % of the spring tide range (4.94 m) respectively.

The scatter plots and histograms shown in Figure 10 and Figure 11 demonstrate that the modelled currents were broadly of the same speed and direction as the observed data. The East component of velocity at the ADCP location was satisfactorily reproduced by the model, with values of the model skill, d_2 , of 0.54, 0.51 and 0.52 for the three selected cell depths (Figure 12). Similarly for the North component of velocity, it was satisfactorily reproduced with model skill values of 0.58, 0.55 and 0.67 at the three selected cell depths. The values of the MAE and RMSE were in the range 2 - 7 cm s^{-1} (Table 3).

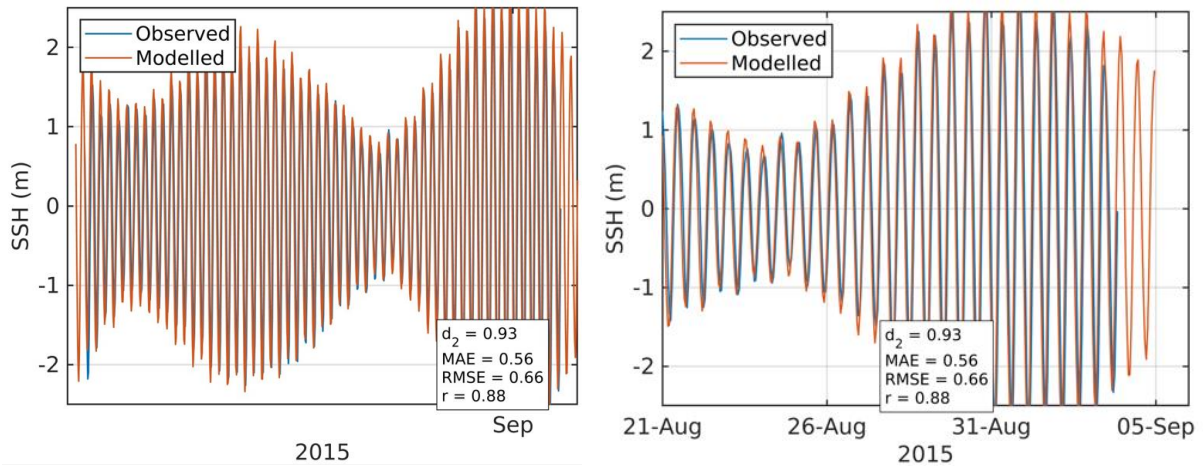


Figure 9. Comparison between observed and modelled sea surface height from January – March 2023 (ADCP deployment ID409) using model parameter values from Table 1. Both the full record (left) and a subset of 15 days (right) are shown. Observed data are in blue, model results in red.

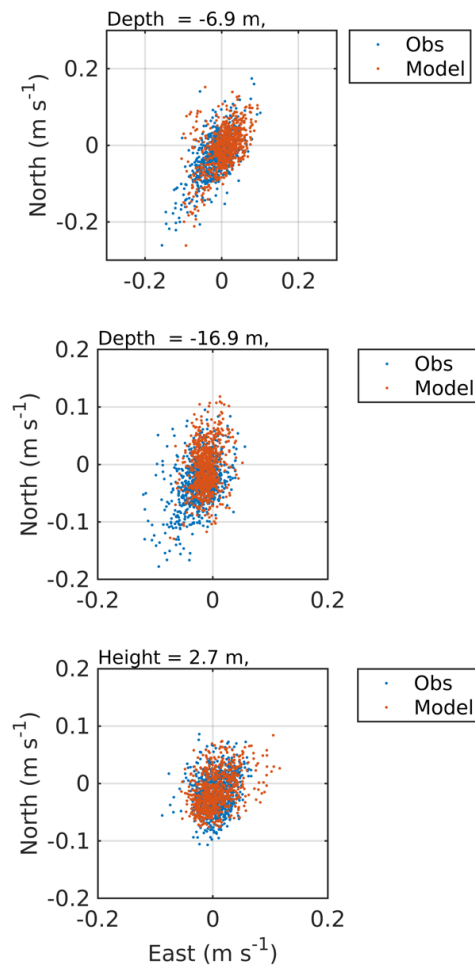


Figure 10. Scatter plots of observed and modelled velocity for the three selected cell depths at the nominal ADCP location for August – September 2015 (ID054). Observed data are in blue, model results in red.

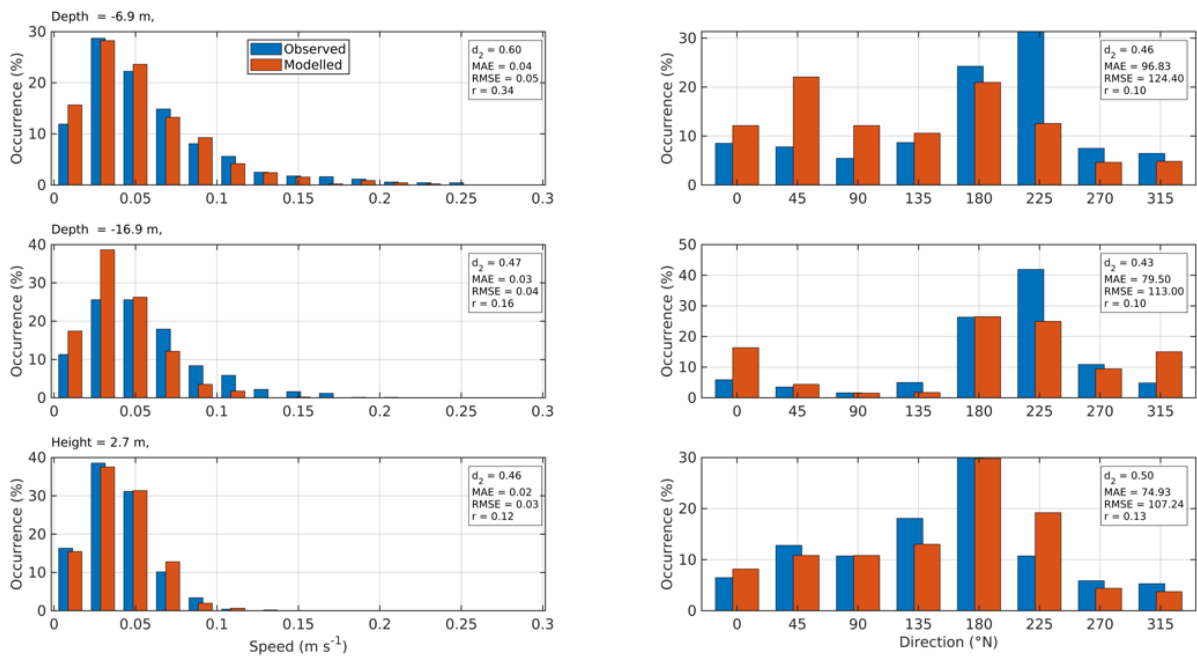


Figure 11. Histograms of observed and modelled speed (left) and direction (right) for the three selected cell depths at the ADCP location from August – September 2015 (ID054). Observed data are in blue, model results in red.

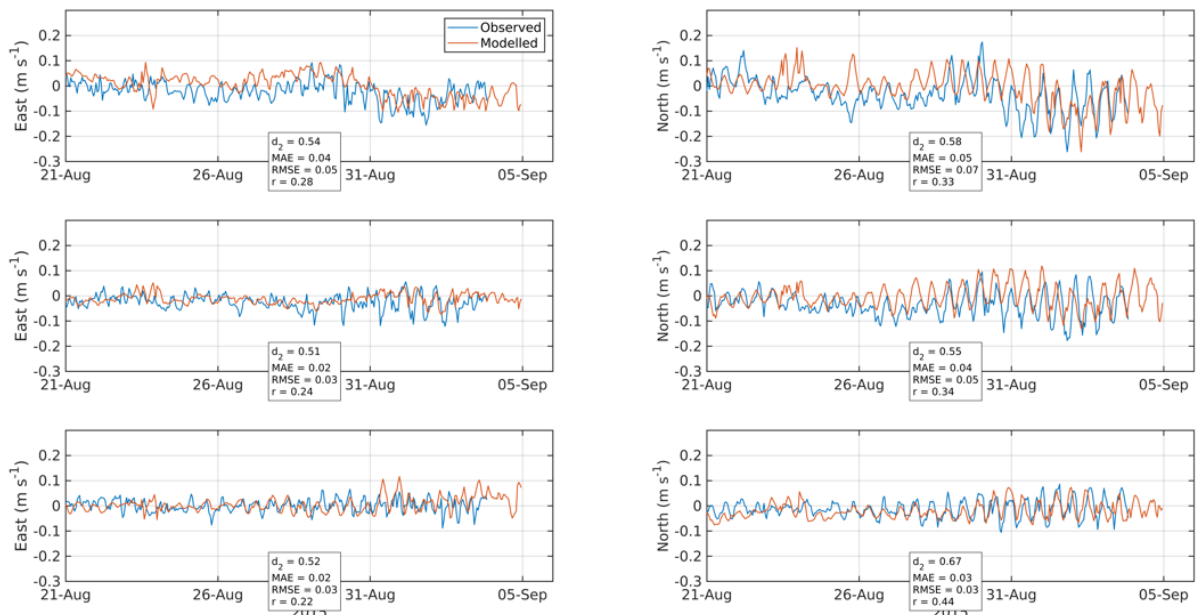


Figure 12. Comparison between observed and modelled East (top) and North (bottom) components of velocity for the three selected cell depths at the ADCP location for August – September 2015 (ID054). Observed data are in blue, model results in red.

Table 3. Model performance statistics for East and North velocity for the three selected cell depths at the ADCP location from August – September 2015 (ID054).

		East	North
Near-surface cell	Model skill	0.54	0.58
	MAE	0.04	0.05
	RMSE	0.05	0.07
Cage-bottom cell	Model skill	0.51	0.55
	MAE	0.02	0.04
	RMSE	0.03	0.05
Near-bed cell	Model Skill	0.52	0.67
	MAE	0.02	0.03
	RMSE	0.03	0.03

5. Modelled Flow Fields, August – September 2015 (ID054)

Modelled flood and ebb velocity vectors at a spring tide on 1st September 2015 are illustrated in Figure 13. The Scalpay site is exposed to strong currents from The Inner Sound, with near-surface flood tide current speeds of up to 25 cm s⁻¹. Mean current speeds are moderate around the Scalpay site, with a mean current speed of about 5 cm s⁻¹.

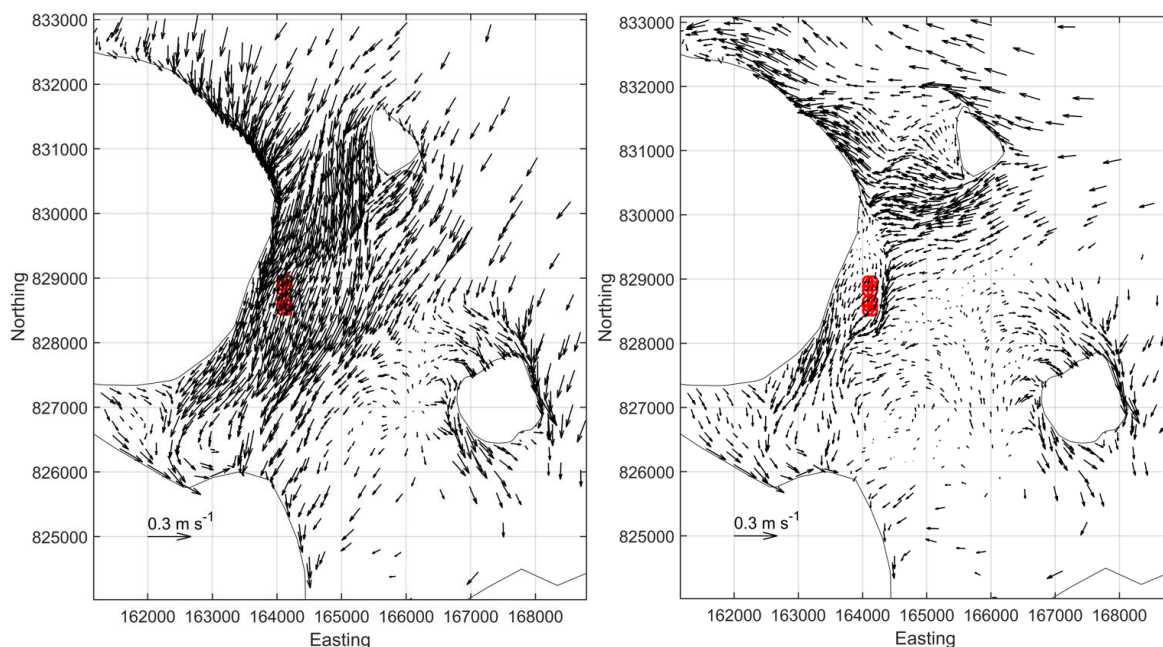


Figure 13. Modelled flood (left) and ebb (right) surface current vectors during spring tides. For clarity, only every 10th vector is shown.

6. Model Evaluation against Dye and Drogue Track Data

Anderson Marine Surveys Ltd. undertook a number of dye and drogue studies at the Scalpay site between 5th and 6th March 2022. The times and locations of the dye releases are detailed in Table 4. For each release, 1 kg of dye was discharged.

6.1 Dye Releases

Table 4. Details of the dye releases undertaken at Scalpay in March 2022

Release	Date	Release Time	Easting	Northing
11A	05/03/2022	07:31:55	164232	828144
11B	05/03/2022	10:02:15	163723	828482
11C	05/03/2022	13:20:20	163765	829166
12	06/03/2022	07:21:30	164322	828204
13	06/03/2022	10:41:35	164320	828192
14	06/03/2022	13:19:15	164320	828187
15	06/03/2022	13:59:15	164333	828170
16	06/03/2022	16:26:10	164341	828177

Following each release, multiple discrete surveys of the dye patch were undertaken. From these data, the location of the centre of the dye patch was estimated over time.

The modelling simulated these releases by releasing particles in discrete patches at the times given in Table 4. Modelled particle locations were recorded every 10 minutes, and the mean particle location (assumed to represent the centre of the patch) was calculated. Particles were released in a 10 m radius circle about the release location over a depth range of 0 – 1 m. The tracks of the modelled particle patch centres (calculated as the mean location of all particles) were then compared to the observed data tracks.

The modelled dye tracks broadly match the tracks of the observed dye releases (Figure 14), with the exception of the first release (shown in red). Dye for the first release (Release 11) was released almost exactly at slack water, which made the initial movements of the dye patch more susceptible to random eddying effects, making prediction of the subsequent dye track more challenging, as the initial movements can significantly affect subsequent displacement. For the subsequent releases (Releases 12 – 16), discharged when the tidal currents were stronger, the modelled tracks are good, generally reproducing both the direction and magnitude of travel.

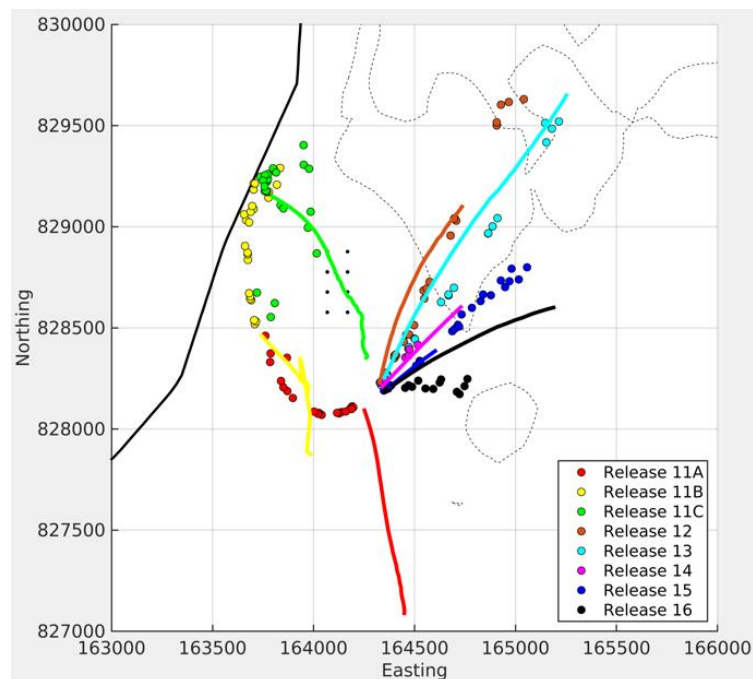


Figure 14. Observed (circles) and modelled (solid lines) dye tracks from the eight releases at Scalpay on the 5th and 6th March 2022. Each release is coloured differently.

6.2 Drogue Releases

The modelling simulated the drogue releases similar to that of the dye patches - by releasing particles in discrete patches at the times given in Table 5. Modelled particle locations were recorded every 10 minutes, and the mean particle location (assumed to represent the drogue location) was calculated. Particles were released in a 10 m radius circle about the release location over a depth range of 0 – 1 m. The tracks of the modelled drogues (calculated from the mean particle location for each release) were then compared to the observed data tracks.

Figure 15 shows the modelled and observed drogue tracks for the releases detailed in Table 5 and confirms that the model broadly matches the tracks of the observed drogues, again with the exception of the drogues released at slack water (ca. 07:30) on 5th March (drogue release 12). The modelled tracks for releases 13 – 16 compared very well with the observed tracks, with only a slight offset in the direction of the Release 15 drogues (Figure 15).

Table 5. Details of the drogue releases undertaken at Scalpay in March 2022. Note that the drogue release numbers do not correspond directly to the dye release numbers.

Release No.	Date	Release Time	Recovery Time	Duration (hrs)
12	05/03/2022	07:30	18:00	10:30
13	06/03/2022	07:20	10:20	03:00
14	06/03/2022	10:38	13:00	02:22
15	06/03/2022	13:18	16:04	02:46
16	06/03/2022	16:24	18:10	01:46

Table 6. Location details for each drogue release

Release No.	Drogue No.	Easting	Northing
12	i	164211	828142
12	ii	164216	828150
12	iii	164207	828143
13	i	164248	828195
13	ii	164303	828213
13	iii	164248	828184
14	i	164266	828189
14	ii	164270	828206
14	iii	164308	828186
15	i	164304	828206
15	ii	164254	828212
15	iii	164276	828208
16	i	164297	828181
16	ii	164259	828169
16	iii	164306	828176

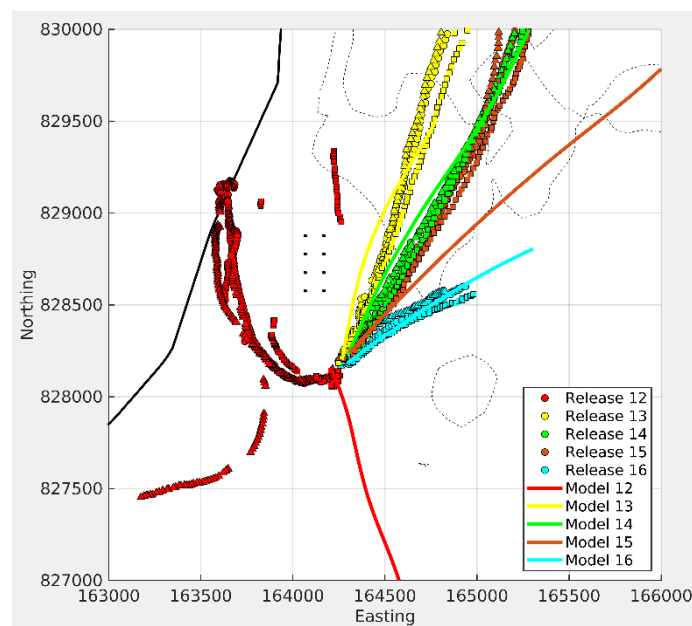


Figure 15. Observed (symbols) and modelled (solid lines) drogue tracks from the eight releases at Scalpay on the 5th and 6th March 2022. The different shaped symbols represent individual drogues.

Given the challenges in modelling short-term dye and drogue tracks in dynamic tidal environments, the comparison shown here between modelled and observed tracks for both dye and drogue releases is considered to be very good, and demonstrates that the hydrodynamic model is capable of providing good predictions of transport pathways and dispersion of wastes discharged into the local marine environment.

7. References

Burchard, H., 2002. Applied turbulence modelling in marine waters. Springer:Berlin-Heidelberg-New York-Barcelona-Hong Kong-London-Milan Paris-Tokyo, 215pp.

Chen, C., H. Liu, and R.C. Beardsley, 2003. An unstructured, finite-volume, three-dimensional, primitive equation ocean model: Application to coastal ocean and estuaries. *J. Atmos. Ocean. Tech.*, 20, 159 – 186.

European Centre for Medium-Range Weather Forecasts (ECMWF) 2021, ERA5 Dataset <https://www.ecmwf.int/en/forecasts/datasets/reanalysis-datasets/era5>

Gillibrand, P.A., Walters, R.A., and McIlvenny, J., 2016. Numerical simulations of the effects of a tidal turbine array on near-bed velocity and local bed shear stress. *Energies*, vol 9, no. 10, pp. 852. DOI: 10.3390/en9100852

Large, W.G. and Pond, S., 1981. Open ocean momentum flux measurements in moderate to strong winds. *J. Phys. Oceanogr.*, 11, 324—336.

Marine Scotland, 2016. Scottish Shelf Model. Part 1: Shelf-Wide Domain. Available at <http://marine.gov.scot/taxonomy/term/1964#:~:text=The%20Scottish%20Shelf%20Model%20%20%20%20,%20%20%20%20%2016%20more%20rows%20>

Mowi, 2024. Azamethiphos Dispersion Modelling Report: Scalpay, Inner Sound. Mowi Scotland Ltd., March 2024, 28 pp.

Pawlowicz, R.; Beardsley, B.; Lentz, S., 2002. Classical tidal harmonic analysis including error estimates in MATLAB using T_TIDE. *Computers & Geosciences*, 28, 929-937.

SEPA, 2023. Interim Marine Modelling Guidance for Aquaculture Applications. Scottish Environment Protection Agency, December 2023, 11 pp.

Walters, R.A.; Casulli, V., 1998. A robust, finite element model for hydrostatic surface water flows. *Comm. Num. Methods Eng.*, 14, 931–940.

Willmott, C. J.; Ackleson, S. G.; Davis, R. E.; Feddema, J. J.; Klink, K. M.; Legates, D. R. O'Donnell, J.; Rowe, C. M. 1985. Statistics for evaluation and comparison of models, *J. Geophys. Res.*, 90, 8995– 9005.